12-2007

Validation of adaptive aeroelastic finite element program for two dimensional flow past a suspension bridge girder section using unstructured grids.

Shanique Murray
University of Arkansas, Fayetteville

VALIDATION OF ADAPTIVE AEROELASTIC FINITE ELEMENT PROGRAM FOR TWO DIMENSIONAL FLOW PAST A SUSPENSION BRIDGE GIRDER SECTION USING UNSTRUCTURED GRIDS.

VALIDATION OF ADAPTIVE AEROELASTIC FINITE ELEMENT PROGRAM FOR TWO DIMENSIONAL FLOW PAST A SUSPENSION BRIDGE GIRDER SECTION USING UNSTRUCTURED GRIDS.

A thesis submitted in partial fulfillment
of the requirements for Honor Studies in Civil Engineering

By

Shanique Murray

December 2007
Department of Civil Engineering
College of Engineering
University of Arkansas

This thesis is approved for
recommendation to the
Honor's College

Thesis Director:

Dr. Panneer Selvam

Thesis Committee:

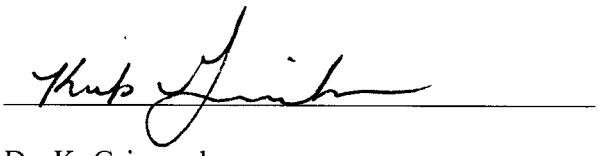

Dr. K. Grimmelsman

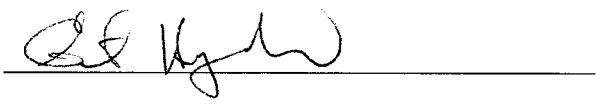

Dr. E. Heymsfield

Thesis Duplication Release

I hereby authorize the University of Arkansas Libraries to duplicate this thesis when needed for research and/or scholarship.

Agreed Shanique Murray
(signature of student)

Refused _____
(signature of student)

ACKNOWLEDGEMENTS

I would like to sincerely thank my honors advisor, Dr. R. Selvam for his guidance and support with this project. I am especially grateful for the financial support through James T. Womble to perform this work. I am thankful for the opportunity to use Dr. Selvam's adaptive finite element program, Tecplot software and Unix machines at the Computational Mechanics Laboratory.

I would also like to thank Dr. Sanjaya Patro for his guidance and assistance with running and understanding the adaptive finite element program. In addition I would like to thank the research group at the Computational Mechanics Lab, especially Mita Sarker, for their assistance with learning the Tecplot software and operating the Unix machines.

My sincere thanks are extended to my honor committee members, Dr. K. Grimmelsman and Dr. E. Heymsfield. I am grateful to Dr. K. Grimmelsman and Dr. E. Heymsfield for time spent reviewing this thesis.

Table of Contents

LIST OF FIGURES

LIST OF TABLES

ABSTRACT

The flow around suspension bridge decks was traditionally investigated using wind tunnel experiments. Computer modeling, an alternative to wind tunnel testing is now being used to simulate the wind flow around a bridge cross section. This alternative is less expensive and takes less time compared to wind tunnel experiments. The motion of flow around a bridge deck is described by a set of partial differential equations called Navier-Stokes (N-S) equations. Flow features such as velocity, pressure and vorticity are predicted by solving these equations. These flow features are then used to compute flow parameters such as aerodynamic drag, lift and moment coefficient; C_d, C_l and C_m and Strouhal number S_t. In 2001, Selvam and Govindaswamy created two computer models. These computer models were used to compute flow parameters using quadrilateral finite elements (structured meshes). The main problem with both computer models was creating a proper grid around the bridge section and controlling the error within the solution. To address this problem, automatic generated triangular grids (unstructured grids) are used in the existing models. Adaptive finite element techniques and error estimation algorithms are also used in the model. Error estimation algorithms determine the error in the FEM mesh. Adaptive techniques remesh the grid around the bridge section whenever the calculated error exceeds a specified limit. In this research, the influence of specified permissible errors and grid sizes on the accuracy of flow parameters (drag coefficient and Strouhal number) is studied. It is found that the computed drag coefficient and Strouhal number for Great Belt East Bridge Section are improved using the adaptive finite element model.

CHAPTER 1: INTRODUCTION

1.1 General Overview

The effect of wind loads on suspension bridges became a major concern for bridge designers after the collapse of Tacoma Narrows Bridge in 1940. A moderate wind storm of 42 mph ripped apart the bridge, buckling the stiffened girders at the mid span (Bowers, 1940). To understand the response of bridges to wind loads, engineers traditionally used wind tunnel experiments to predict the aerodynamic responses of new bridge designs to various wind speeds. However, these experiments are expensive and time consuming (Larsen and Walter, 1996). A typical wind tunnel test can generally take 6 to 8 weeks to perform a single experiment. The cost of performing this test can range from $50,000 to $100,000 per bridge girder cross section (Selvam, 2003). Nowadays, with the advances in computer technology and numerical modeling, the interaction of wind around a bridge deck can now be more readily simulated using computer models. In addition, aerodynamic responses can be predicted more quickly. This chapter presents an overview of the project and states the objective of the project

The governing equations for fluid flow around a bridge deck are the Navier-Stokes equations. These equations are very complex and highly nonlinear. Traditionally, numerical techniques such as the Finite Element Method and Finite Difference Methods have been used to approximate the solutions to the Navier-Stokes equations. In these techniques, the domain of the problem is divided up in to small areas/volumes (“grids”) and the solutions to the Navier-Stokes equation are solved for each element; however, these approximation techniques introduce errors in the solution.

The Computational Mechanics Laboratory at the University of Arkansas has recently developed a two dimensional fixed grid (UABRIF) and a moving grid (UABRIM) finite element computer program to analyze flow field around a suspended bridge deck cross-sections (Selvam et al., 2001). Testing of this program was conducted by Govindaswamy (2001) and Gazel (2004). Govindaswamy's research used the Great Belt East Bridge (GBEB) suspension bridge to perform the FEM analyses. UABRIF was used to compute the aerodynamic force and moment coefficient; C_d, C_l and C_m for a fixed grid. In the fixed grid case, the bridge cross-section is assumed to be rigidly fixed and is restrained against any rotational or translational displacements. UABRIM was used to compute the critical velocity for flutter for a moving grid. In the moving grid case, bridge section is allowed to rotate freely about the shear center; this motion is known as pitching. In addition the bridge is allowed to translate along it center of gravity; this is referred to as heave.

In Govindaswamy's (2001) research, GBEB bridge section was modeled . Govindaswamy (2001) generated four different grids using UABRIM and compared results from each grid. For each grid, Govindaswamy varied the grid sizes around the bridge section. Gazel investigated numerical instabilities inherent in the computer codes and applications of the computer program to other bridge deck geometries. Both researchers found that the values of the drag force coefficient, Strouhal number and critical velocity were in good agreement with wind tunnel test results for GBEB Bridge. The main challenge with this model is creating proper meshes around the bridge deck. Researchers spent a great deal of time creating an efficient grid around the bridge section.

A proper grid is needed to enhance the grid resolution of local flow features such as pressure around a bridge.

The Computational Mechanics Laboratory is currently involved in improving the computer model so that it is more user-friendly and has better control of the accuracy. The previous models solved the Navier-Stokes equations using the finite element method on a structured grid (quadrilateral elements). The improved computer program model solves the Navier-Stokes equation on unstructured grids (triangular elements). Error estimation techniques and adaptive techniques are implemented into the improved computer model to control the error in the FEM mesh and to refine the regions where there is more error.

In the adaptive remeshing, the errors are first calculated to asses the accuracy of the solution. If the errors are larger than the error tolerance, the finite element model is then refined by using adaptive techniques. The grid is then re –analyzed and the errors in the new grid are recalculated. The procedure is continued until the calculated errors fall below the specified permissible values. Thus, adaptivity means that the FEM model refinement depends on the error distribution (Selvam and Qu, 2002).

1.2 Objective of Report

The objective of the research is to investigate the improved finite element model. The wind tunnel data from the Great Belt East Bridge (GBEB) will be used to validate results from the improved model. Data from other recent computational models will also be used to evaluate and compare this new model. This objective will be achieved through the following steps:

1. Understand 2D – automatic unstructured grid generation using advancing front method.

2. Understand h-adaptive finite element method with respect to fluid flow problem.
3. Prepare a user manual that describes the input file.
4. Run the program changing input parameters: grid spacing and overall percentage of error over the region.
    a. Determine the lowest error that a user can prescribe within the model
    b. Determine flow parameters for each run
5. Use the tecplot software to evaluate wind flow features around bridge section considering adaptive automatic grid generation algorithm.
6. Compare and validate computed flow parameters against wind tunnel experiment and the results from computer models that used the same GBEB section. The documented results used to validate and compare results are generated from Govindaswamy's (2001), Larsen et al (1997), Taylor et al. (1999) and wind tunnel experiment.
7. Discuss the limitations of using the model.

A review of the performance of this new program will assist engineers in using the computer model more effectively. With this information, designers will be able to:

- Determine the minimum error that can be used with this model for specified grid resolution
- Understand the influence of prescribed errors on the accuracy of drag coefficients, and Strouhal number
- Understand the influence of grid sizes on accuracy of drag coefficients and Strouhal number

1.3 Organization of Report

This report is organized in the form of chapters. The introduction gives an overview of the project and states the objective of the project. Chapter two presents an overview of bridge aerodynamics. In chapter three, a literature review of adaptive techniques and error estimation used in modeling flow is presented. Chapter four presents issues in computer modeling. Chapter five presents an overview of the grid generation procedure and adaptive remeshing used in the improved model. Chapter six presents the results and outcome of the research. Chapter seven concludes the research and provides recommendations for future work.

CHAPTER 2: LITERATURE REVIEW: BRIDGE AERODYNAMICS

2.1 Introduction

The area of bridge aerodynamics was initiated after the collapse of the Tacoma Narrows Suspension Bridge in 1940. The Tacoma Narrows Suspension Bridge is located in the state of Washington. The bridge had a span of 2800 feet (Farren, 1999). A moderate windstorm of 42mph caused a dynamic fluid structure interaction which resulted in the bridge experiencing large amplitude vibrations. This caused the suspender cables to fail and the roadway to fall into the water. The Tacoma Narrows Bridge failure was due to dynamic phenomenon called flutter (Huston and Bosch, 1996). As a result of this failure extensive research has been carried out to better understand the response of long span bridges under wind excitation. Better understanding of responses of bridge decks to wind forces can assist engineers in creating safer designs for bridges.

Two issues considered for safer designs of bridges are (i) static behaviors: overturning, excessive lateral deflection and lateral buckling, (ii) dynamic behaviors: vortex shedding, self excited oscillation (flutter) and buffeting by wind turbulence. Usually static behaviors are not as critical for design of bridges as oppose to dynamic behavior of bridges. Static behaviors are usually checked by solving aerodynamic force components such as lift force, drag force and pitching moment. The dynamic behavior of bridges is more important in the design of bridges because they can lead to fatigue failure.

When a bridge is subjected to wind flow, it may oscillate or suddenly deflect. The structural motion of the bridge causes changes in the flow pattern around the bridge. The

change in the flow pattern increases the vibration, thereby giving rise to succeeding deflection.

Researchers used experimental methods such as wind tunnel experiments and computational methods to model the aerodynamic behavior of the bridge during the wind storm. Combinations of wind tunnel testing and computer modeling are used to predict the pressure exerted on a new bridge design due to wind loading. The objective of these technologies is to present the engineer with results that can predict reliably the response of such sophisticated structures (Farren, 1999). In this chapter, an overview of both approaches used to analyze the performance of a bridge under wind loading is presented.

2.3 Wind Tunnel Experiments

The effect of wind on a suspension bridge is traditionally modeled using wind tunnel experiments. Wind tunnel testing involves the construction of models of the structure and the surrounding buildings. These models are tested in wind tunnels and other facilities (Cengel, 2003). The instantaneous pressure and force exerted on a model during testing is measured.

There are three types of wind tunnel tests used on suspension bridges (Farren, 1999). These are as follows:

- Models of the entire bridge
- Taut strip models
- Sectional models

Modeling the entire bridge allows the engineer to compare a model that is identical to the structure. However these models are expensive to build. Previous designs indicate a scale

of 1:300 is desirable. The distribution of mass in these models is identical to the mass distribution of the real structure (Farran, 1999)

Taut strip models consist of two wires that are stretched across the wind tunnel. The response of these models to wind flow is similar to the response of the center section on the suspension bridge (Farren, 1999).

The third model is made of sections of the bridge deck section in the span –wise direction. The ends of the section are supported on a spring type foundation that allows rotation and motion in the vertical direction. In addition these models are used to investigate coefficients for drag, lift and moment (Farran, 1999).

2.4 Computational Methods

Numerical simulations of wind flow around bridge section involve solving the Navier-Stokes equations. The Navier-Stokes equations describe the motion of the fluid. The solutions to N-S equations consist of components of velocity, pressure and vorticity. The solutions to fluid equations are used to determine flow parameters for a bridge section. The flow parameters for a bridge section are discussed in chapter four.

2.5 Techniques for Modeling the Wind Flow

These equations are approximated by using techniques like finite element method (FEM), finite difference method (FDM), discrete vortex method (DVM) and finite volume method (FVM). The turbulence in the flow is modeled using turbulence models. The solution is based on a grid that is generated in the domain of the fluid around the structure.

Researchers such as Larsen and Walther (1997) used a viscous DVM to compute flow parameters for the flow around the Great Belt East Bridges (GBEB). Larsen and Walther found that their flow parameters were in reasonable agreement with wind tunnel tests.

FEM and FDM approximates the unknown into the set of simultaneous equations of the type AX=B. These equations can be solved by many procedures like Gauss-elimination; Gauss- Seidal and Preconditioned conjugate (PCG) methods. FDM takes less computational time and storage space than FEM. However the FDM is geometrically restrictive whereas FEM is good for complex geometrical shapes.

2.7 Turbulence Models

For turbulent flows, turbulence models are also used to model the turbulence in the flow. Turbulence modeling issues were discussed in detail in Selvam (1998& 1999). Widely used turbulence model include the Reynolds Averaged Navier- Stokes (RANS), Large Eddy Simulation (LES) and Vortex Methods (VM).The turbulence model used in previous works is the large eddy simulation model. Selvam et al. (1997 to 2001), Fransen and McRobie (1999), Enevoldsen et al. (1999) and Hansen et al. (1999) used LES turbulence modeling to compute flow parameters for the GBEB approach and suspension span.

CHAPTER 3: LITERATURE REVIEW: ADAPTIVE MESH REFINEMENT AND ERROR ESTIMATION

3.1 Introduction

Wind flow around bride deck section using finite element method has been illustrated in the previous model (Selvam 2000, 2001). Researchers checked the accuracy of the FEM model by comparing the FEM solution with wind tunnel experiments. The mesh was redesigned based on that error. Originally, designers ran the analysis on several meshes with different grid sizes to achieve more accurate results. However, the process of trial and error took considerable time. Error Estimation and Adaptive refinement techniques can be used to reduce the computer time and storage while maintaining a desired accuracy. The process works such that the grid is constantly remeshed based on a specified permissible error. This chapter presents a discussion on error estimation and adaptive techniques in finite element computations.

3.2 Error Estimation

Error estimation is based on modified version of the following two approaches. The first approach was introduced by Babuska and Rheinbodlt in 1978. Their approach considers local residuals (errors) in the numerical solution. They begin by investigating the overall error occurring in a patch of elements and then in a single element. The second approach is based on a stress–recovery technique called “best guess stress methods”. This technique was later updated by Zienkiewicz and Zhu (1987). The best guess stress approach is used in the improved finite element method.

3.3 Best Guess Stress Method

Zienkiewicz –Zhu have developed an error estimator that uses error norms. The most frequently used norm is the energy norm $\|e\|$. Zienkiewicz and Zhu evaluate the error energy norm from the expression (Zienkiewicz and Zhu 1987),

$$\|e\| = \left(\int_{\Omega} \left(\sigma^* - \sigma'\right)^T D^{-1} \left(\sigma^* - \sigma'\right) d\Omega \right)^{1/2} \tag{3.1}$$

In this expression: σ^* = best guess stresses, σ' = stresses from FE solution, D = elasticity matrix, Ω = Domain under consideration.

The best guess values for (3.1) can be determined in several ways: nodal averaging, least squares smoothing, and Loubignac iteration (Hinton et al. 1991).

The best guess stress values are evaluated considering nodal averaging stresses for 3-noded triangular element.

$$\sigma^*_{element} = \frac{\sigma_1' + \sigma_2' + \sigma_3'}{3} \tag{3.2}$$

$\sigma^*_{element}$ = Smooth stress at each element, $\sigma_1', \sigma_2', \text{and} \, \sigma_3'$ are FE stresses at respective nodes of 3-noded triangular element.

3.4 Adaptive Finite Element Refinement

Adaptive finite element refinement can be summarized as follows. First the errors in each element would be estimated and then total error in the domain is estimated. The simplest process to keep the total error within permissible value is an equal error distribution between all elements. Considering the total permissible error, the error can be divided between the existing number of elements used and it is then found whether more

refined elements need to be used. In general, three different families of refinement strategies have been considered to date (Lohner 2001):

1. Mesh movement or Repositioning (R – methods)
2. Mesh enrichment (H/P – Methods)
3. Adaptive re-meshing (M – Methods)

3.4.1 Mesh Movement or Repositioning (R – methods)

This technique involves repositioning points in the field without changing the element topography (point connectivity) (Lohner 2001).

3.4.2 Mesh Enrichment (H/P – Methods)

In this technique, degrees of freedom are added or taken from the mesh. The element may either split into new ones (h-refinement) or add further degrees of freedom with hierarchical shape function (p-refinement) (Lohner 2001).

3.4.3 Adaptive Re-meshing (M – Methods)

This technique came into existence after the development of the automatic mesh generators. The mesh generator is used in combination with an error indicator to re- mesh the computational domain either globally or locally, to produce a more suitable discretization (Lohner 2001).

3.5 Previous Work Done Using Adaptive Finite Element

Choi and Yu (1998) investigated the h-refinement for flows over a square cylinder. They used the penalty-function formulation to solve the NS equations. This procedure is not used commonly in Computational Wind Engineering Problem. Selvam et

al. (2002) applied the mesh enrichment technique (h-refinement) and p-refinement techniques to flows over a circular cylinder. He used the primitive variable form to solve the NS equations.

Selvam and Zu-Quing Qu have implemented both a p-version and h-version adaptive finite element technique into a computational flow problem. In their paper, the error distribution of the vorticity was first estimated. The degree of freedom for the shape function of the elements is changed and the grids are refined simultaneously.

CHAPTER 4: COMPUTER MODELING

4.1 Introduction

Computer modeling for flow around GBEB bridge section has been illustrated in previous works (Selvam, 2002). Many researchers have worked on the Great Belt East Bridge (GBEB) section because there are extensive wind tunnel results against which their computer model could be validated. Selvam (1998), Selvam & Bosch (1999), Selvam and Govindaswamy (2001), Frandsen and McRobie (1999) used computer modeling to compute the flow around the GBEB section. In this chapter the concepts relating computer modeling are discussed. Boundary conditions used in solving the Navier-Stokes equations are also presented.

4.2 The Structure

The cross section of the Great Belt East Bridge (GBEB) suspension span shown in figure 4.1 was used in this simulation process as well as in previous works.

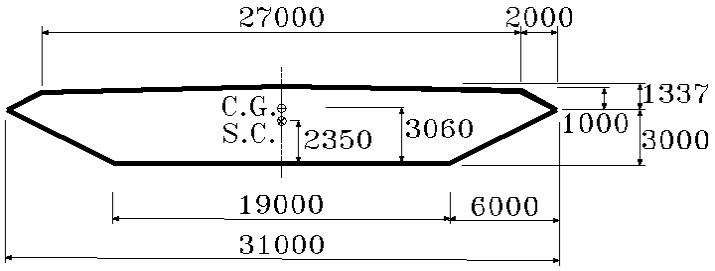

Figure 4.1: Cross section of the GBEB suspension span
(All dimensions are in mm)

The GBEB is a 3 span box girder suspension bridge of span lengths 535m-1624m-535m. This bridge carries a four lane motor way across the international shipping route of the Great Belt, Denmark (Larsen et al 1999).

Structural properties of the GBEB Bridge are shown below (Larsen, 1996).

Mass (Kg/m) = 2338.100

Inertia (Kgm^2/m) = 261.820

Frequency of heave oscillation Fh (Hz) = 0.099

Frequency of pitch oscillation Fα (Hz) = 0.272

4.3 Flow Parameters

The flow parameters that characterize flow are the Reynolds number (R_e), Strouhal number (S_t) and coefficient of drag force (C_d) and coefficient of lift force (C_l). These flow parameters are described as follows:

$$R_e = \frac{VB}{\upsilon} \tag{4.1}$$

$$S_t = \frac{H}{TV} \tag{4.2}$$

$$C_d = \frac{F_x}{0.5\rho V^2 B} \tag{4.3}$$

$$C_l = \frac{F_y}{0.5\rho V^2 B} \tag{4.4}$$

Where B, H are the width and height respectively, Fx, Fy the drag and lift forces, V the reference velocity , υ the kinematic viscosity, and T the period of the oscillation of the lift forces and ρ is the density. (Selvam, Bosch and Govindaswamy, 2002).

4.4 Governing Equations of Flow

The motion of flow around a bridge is described by a set of coupled differential equations called Navier-Stokes (N-S) equation. The Navier-Stokes equations consist of a continuity equation for conservation of mass and three time-dependent conservation of momentum equations. The Navier-Stokes equations are unsteady, nonlinear, second order, partial differential equation that has four unknowns (three velocity components and pressure). The two dimensional equations for an incompressible flow written in general tensor notation are as follows:

Continuity Equation: $$U_{i,i} = 0 \tag{4.5}$$

Momentum Equation: $$U_{i,t} + U_j U_{i,j} = -\left(p/\rho\right)_{,i} + \left[\nu\left(U_{i,j} + U_{j,i}\right)\right]_{,j} \tag{4.6}$$

where

U_i =velocity in the i[th] direction

p = pressure

ρ = fluid density.

A comma represents differentiation; t represent time. i =1 and 2 mean variables in the x and y directions. In the previous model, another equation was used to implement higher order approximation of the convection term. This equation is used instead of Equation 4.6

$$U_{i,t} + U_j U_{i,j} - \theta\left(U_j U_k U_{i,j}\right)_{,k}/2 = -\left(p/\rho\right)_{,i} + \left[\nu\left(U_{i,j} + U_{j,i}\right)\right] \tag{4.7}$$

According to Selvam and Govindaswamy (2002), "depending upon the values of θ, different procedures can be implemented to solve the equation. For balance tensor

diffusivity (BTD) scheme, $\theta = \delta t$ was used; where δt is the time step size used in the integration. For streamline upwind procedure suggested by Brooks and Hughes (1982), θ is considered as

$$\theta = \frac{1}{\max\left(\frac{|U_1|}{dx}, \frac{|U_2|}{dy}, \frac{|U_3|}{dz}\right)} \tag{4.8}$$

In this equation, dx, dy, and dz are the control volume length in the x, y, and z directions and U_1, U_2, and U_3 are the velocities in the three directions. In the previous model $\theta = \delta t$ was used (Selvam, 2002.).

4.5 Boundary Condition

Boundary conditions are specified at each edge of the computational domain (2-D) flows. Figure 4.3 shows the schematic representation of the domain chosen for the problem and the boundary conditions applied in the computations. In figure 4.3, B represents the width of the bridge.

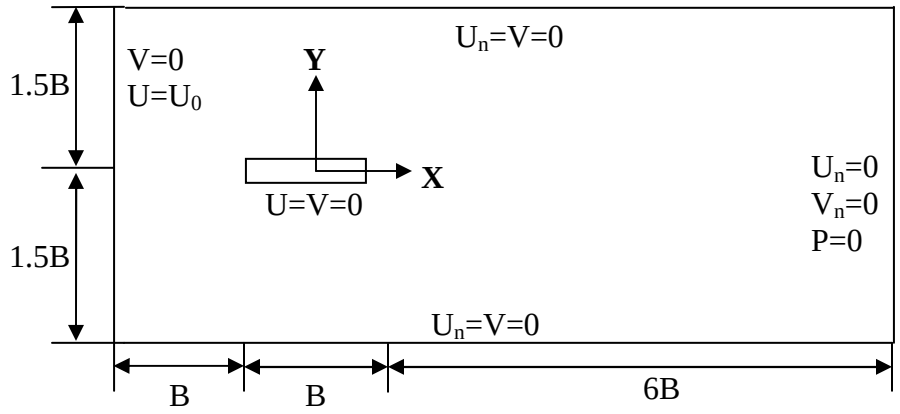

Figure 4.2: Solution domain and the boundary conditions

Boundary Condition (FIXED BRIDGE):

- Inlet velocities in the x and y directions are considered to be one and zero respectively.
- The vertical velocities on the top and bottom sides of the computational regions are considered to be zero (no slip condition)
- The velocities in the x and y direction are considered to be zero on the surface of the bridge.
- The pressure is considered zero

4.6 Finite Element Solution Scheme to Solve the Navier Stokes (N-S) Equations

The governing equations are solved on the grid domain by the finite element methods (FEM) and the turbulence is modeled using the large eddy simulation (LES). The N-S equations are solved using an iterative implicit method suggested in Selvam (1998). This process is carried out by the fluid solver program. The grid is updated based on the result given by the fluid solver. From this procedure, velocity, vorticity and pressures are solved for at each node.

The number of iterations performed depends on the duration of time and time step specified by the user performing the analyses. The time step is specified in the input file.

CHAPTER 5– GRID GENERATION AND ADAPTIVE REMESHING

5.1 Introduction

Previously Selvam et al. (2001), discretized the flow region around the GBEB section into quadrilateral elements using algebraic procedures. The flow region is shown in figure 5.1. The previous model took a great deal of time creating a grid that produces results comparable with wind tunnel. Therefore a more sophisticated grid generation and adaptive procedure is used for computing efficiently.

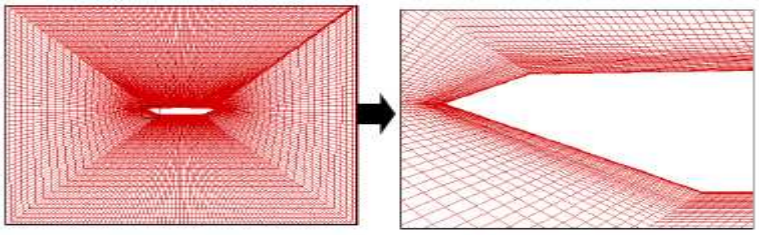

Figure 5.1: The FEM grid system of the GBEB suspension

In this chapter, an overview of the grid generation procedure used in the improved model is presented.

5.2 Computational Grid

Grid generation can be classified into two groups as structured or unstructured grids (Peraire, Morgan, 1990)). We identify two directions within the mesh by associating a coordinate system called ξ, η system or IJ system in mesh lines. The grid lines are the lines of constant ξ or lines of constant η. The node point is formed (ξ, η) with the intersection of grid lines ξ and η. Typically, quadrilateral or hexahedral elements are common in the structured type of meshes (Peraire, Morgan, 1990). In a structured

mesh, each interior nodal point is surrounded by exactly equal number of adjacent elements. For example, in the case of two dimensional problems there are 8 nodes around each interior node. This can be shown in figure 5.2.

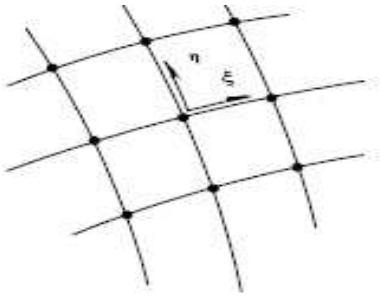

Figure 5.2: Structured mesh discretization

In contrast, in unstructured meshes the number of cells surrounding a typical node is not always constant. This can be shown in Figure 5.3 In the case of unstructured grids the number of nodes surrounding a node will vary in the case of finite element applications. Connections from point to point are listed instead of the IJ system that is used in the structured mesh. The unstructured grid is illustrated in Figure 5.4. The nodes and the elements are numbered and the number of node which belongs to each element is stored (Peraire, Morgan, 1990). Triangle and tetrahedral meshes are the most common types of elements found in unstructured meshes. The principle advantage of the unstructured grid is the ease at which complex domains can be discretized.

Figure 5.3: Unstructured mesh discretization

Element	Nodes		
1	5	8	9
2	9	8	12
3	8	7	12
4	6	7	8
5	5	6	8
6	5	9	10
7	11	5	10
8	3	5	11
9	3	4	5
10	1	4	3
11	4	6	5
12	1	6	4
13	1	2	6
14	2	7	6

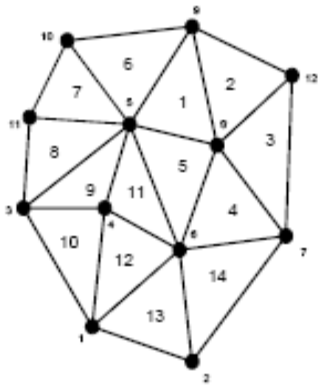

Figure 5.4: Connectivity array for an unstructured triangular mesh

5.3 Issues in the Grid Generation Process

The density and distribution of the grid lines determines the accuracy with which the model represents the actual physical body. For the finite element model employed, the node spacing is denser around to the bridge deck than the boundary. This is because the pressure and velocity gradients are higher around the bridge deck than the boundary. Closer spacing of the nodes around the bridge deck yield more accurate results (Selvam, 2001).

For fluid flow problems, we are dealing with thousands of elements; hence grid generation programs are used to create the elements and nodes. The grid generation program gives the x and y coordinates of each node. In the case of unstructured grids, it also gives the connectivity values of each element. The grid program is implemented into the FEM program. Once the grid is generated; the domain is divided into small elements called cells. For two dimensional (2-D) domains, the cells are called areas.

5.4 Structured Grid Generation Programs

In the previous model, Selvam and Govindaswamy used an in–house structured grid generation programs to construct quadrilateral elements around the bridge section. The grid generation program used to generate the two dimensional fixed grid is called the University of Arkansas Bridge Fixed Bridge (UABRIF) and the program used to create the two dimensional moving grid is called the University of Arkansas Bridge Moving Bridge (UABRIM) grid generation program. Both programs created the grid and performed the Finite Elements Analysis for the bridge deck. For our purposes, we are only concerned with the UABRIF Grid program. The UABRIF program held the bridge deck cross section in a fixed position and computed the drag and lift coefficients .Input data for UABRIF program comprised of the number of nodes and elements in the domain boundary conditions for elements along the boundary of the bridge cross section and the wall of the domain, inverse of the Reynolds number (viscosity of the fluid), duration of time and grid data (x and y coordinates of each node and nodal connectivity of each element). The duration of time is the amount of time during which the flow is simulated and it dictates the number of time steps to be executed (Selvam, 2002).

5.5 Unstructured Grid Generation Programs

In this work an unstructured grid generation program is used in the existing model. This type of generation is used because the problem of generating a mesh over a two dimensional region of complex shape is considerably simplified if unstructured grid triangular meshes are used.

In the unstructured grid procedures the popular grid generation technique are advancing front method and the Delaunay triangulation technique (George, 1992). In the advancing front technique the grid is created from the boundary to all places where there is no grid. The development of the advancing front mesh generation method is described in a series of papers by Peraire and Lohner. It was originally described by Lohner (1985) In the Delaunay triangulation technique an existing grid is modified by new introducing points.

5.6 Automatic Mesh Generation Technique Used in the Project

According to the latest report submitted by Selvam, 2007, the advancing front method is used as the grid generator. Selvam et al (2006) have used advancing front generation algorithm to build meshes containing simple linear triangular elements. The characteristic feature of this algorithm is that the boundary of the problem domain is discretized first and then the elements and nodes are created simultaneously.

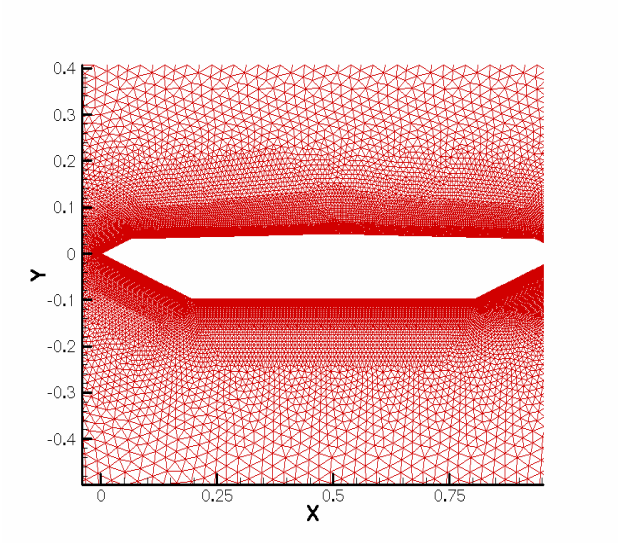

Figure 5.5: Unstructured Grid for GBEB suspension span section

5.6.1 Grid Generation Procedure

The process is started by constructing by hand the course background grid of three node triangular elements which completely covers the domain of the problem. Then define the background nodes and the coordinates of the background nodes of the domain to be discretized. In figure 5.6, the number of element in the back ground grid is 6 and the number of nodes in the background grid is 7. The number of nodes (NN) and number of elements (NE) of the background grid are used as input data into the program. In addition the node spacing around each node in the background grid has to be specified. These parameters (NN, NE) are used as input value for creating of the background grid. Refer to Appendix A for user manual for the adaptive grid generation program.

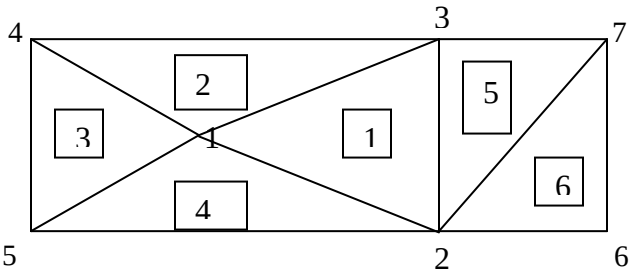

Figure 5.6: Triangle node and element numbers used for the background grid

Next, define the boundary of the domain to be discretized. The boundary of the solution domain is represented by the union of closed loops of curved segment and nodes are placed at points of intersection of these segments. The segments of the exterior boundary are defined in an anticlockwise manner while the segments of the interior boundaries are specified in a clockwise fashion. Figure 5.7 illustrates nodal numbering of the boundary (NN for boundary =13). Before the program can start the process of generating triangles within the region of interest, the positioning of nodes (x and y coordinates) on the boundaries of the region has to be established as well. Number of nodes and x and y coordinates of boundary nodes are also used as input data.

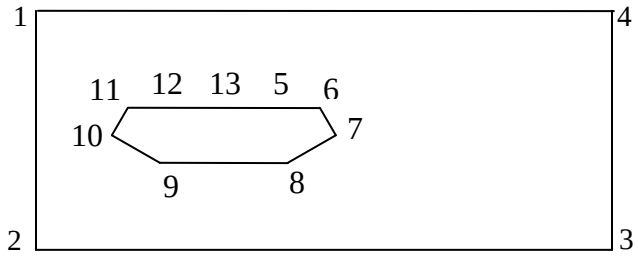

Figure 5.7: Computational domain - Node Number for boundary information

5.7 Error Estimation Used in this Work

The posterior error estimator (best guess stress method) is adopted in this research. According to Selvam et al (2006), the norm of the velocity gradients is defined as:

$$\|\nabla a\| = \left[\int_{\Omega} \nabla u \cdot \nabla u \, d\Omega + \int_{\Omega} \nabla v \cdot \nabla v \, d\Omega\right]^{1/2}, \tag{5.1}$$

In the above equation ∇u and ∇v are the exact velocity gradients. Ω = Domain under consideration. The velocity gradients and their dot products can be expressed as below:

$$\nabla u = i\frac{\partial u}{\partial x} + j\frac{\partial u}{\partial y}, \; \nabla v = i\frac{\partial v}{\partial x} + j\frac{\partial v}{\partial y} \tag{5.2}$$

$$\nabla u \cdot \nabla u = \left(\frac{\partial u}{\partial x}\right)^2 + \left(\frac{\partial u}{\partial y}\right)^2, \; \nabla v \cdot \nabla v = \left(\frac{\partial v}{\partial x}\right)^2 + \left(\frac{\partial v}{\partial y}\right)^2 \tag{5.3}$$

Equation 5.2 is used to evaluate exact velocity gradients analytically.

$$\nabla u_i^* = \frac{\nabla u_1^{'} + \nabla u_2^{'} + \nabla u_3^{'}}{3} \tag{5.4}$$

∇u_i^* = Smooth continuous gradient for *u*-velocity at each element, $\nabla u_1^{'}, \nabla u_2^{'}, \text{and} \nabla u_3^{'}$ are discontinuous gradients obtained from the finite element solution at respective nodes of 3-noded triangular element. Similarly ∇v_i^* = smooth continuous gradient for *v*-velocity at each element can be evaluated respectively. The smooth continuous gradients ∇u^* and ∇v^* can be used to approximate Eq. (5.1) for evaluation of norm of the smooth velocity gradient ∇a^* in the whole domain as,

$$\left\|\nabla a^*\right\| = \left[\int_{\Omega} \nabla u^* \cdot \nabla u^* \, d\Omega + \int_{\Omega} \nabla v^* \cdot \nabla v^* \, d\Omega\right]^{1/2} \tag{5.5}$$

The smooth continuous gradients at each element, *i* numerically evaluated as:

$$\left\|\nabla a_i^*\right\| = \left[\left(\nabla u_i^* \cdot \nabla u_i^*\right) * A_i + \left(\nabla v_i^* \cdot \nabla v_i^*\right) * A_i\right]^{1/2} \tag{5.6}$$

Numerically the norm of velocity gradient can be evaluated as below,

$$\left\|\nabla a^*\right\| = \left(\sum_{i=1}^{NEL} \left\|\nabla a_i^*\right\|^2\right)^{1/2} \tag{5.7}$$

where *NEL* = total number of elements in the domain
Then, Selvam and Patro (2006) obtained an approximation of the error using the posteriori error estimator proposed by Zienkiewicz and Zhu (1987) and numerically, norm of the error in velocity gradient at each element, *i* can be evaluated as:

$$\left\|e_i^*\right\| = \left(\left((\nabla u_i^* - \nabla u_i^{'}) \cdot (\nabla u_i^* - \nabla u_i^{'}) * A_i\right) + \left((\nabla v_i^* - \nabla v_i^{'}) \cdot (\nabla v_i^* - \nabla v_i^{'}) * A_i\right)\right)^{1/2} \tag{5.8}$$

In above equation $\nabla u_i^{'}$ and $\nabla v_i^{'}$ are the discontinuous approximated gradients, obtained from the finite element solution while ∇u_i^* and ∇v_i^* are defined as at above, A_i = area of triangular element, and e_i = approximate error in each element. The dot products in Eq. (5.8) can be expressed as below:

$$\left(\nabla u^* - \nabla u^{'}\right) \cdot \left(\nabla u^* - \nabla u^{'}\right) = \left(\frac{\partial u^*}{\partial x} - \frac{\partial u^{'}}{\partial x}\right)^2 + \left(\frac{\partial u^*}{\partial y} - \frac{\partial u^{'}}{\partial y}\right)^2 \tag{5.9}$$

Also estimate the global error in the whole domain,

$$\left\|e^*\right\| = \left(\sum_{i=1}^{NEL} \left\|e_i^*\right\|^2\right)^{1/2} \text{ where } NEL = \text{total number of elements in the domain.} \tag{5.10}$$

and an average error ρ can be defined by the expression,

$$\left(\sum_{i=1}^{NEL} \left\|e_i^*\right\|^2\right) = NEL * \rho^2 \tag{5.11}$$

The percentage error in the solution can then be evaluated as,

$$\eta = \frac{\left\| e^* \right\|}{\left\| \nabla a^* \right\|} \tag{5.12}$$

This is the procedure that is used in the program to evaluate the error in the velocity gradients. After the error has been evaluated, an adaptive refinement technique is used to refine of the grid so that the new calculated error falls within the prescribed limits

5.8 Adaptive Technique Used in this Work

In the updated UABRIF model, adaptive h- refinement procedures are used to refine the FEM model. The adaptivity criterion is based on an estimate of error in the velocity gradients. This adaptive re-meshing technique allows the overall percentage velocity gradient norm error within a prescribed tolerance and the refinement of the finite element mesh is achieved by generating a new mesh when the discretized error exceeds the tolerance. The user specifies the minimum and maximum grid sizes for element near the bridge deck. The program will only use the specified range of grid sizes to refine the grid.

5.9 Process of Adaptive Mesh Refinement

The AMR procedure is usually based on the following algorithm (Hinton et al. 1991):

1. Generate a initial mesh and carry out an initial FE analysis
2. Based on the results of the FE analysis evaluate the error in the FE solution
3. If the error is within permissible limit then stop; otherwise continue
4. Using any automatic mesh generator algorithm re-mesh based on the information from the error estimator
5. Carry out a further FE analysis based on the new mesh and go to step 2

It can be seen in step 4 that some information is needed by the mesh generator. This information is given in the form of a distribution of new element sizes or spacing, δ_{new} throughout the domain. The values of δ_{new} are specified at the nodes of the current mesh, which then becomes the background mesh for the generation of an entirely new mesh. In this process elements are generated one by one along the generation front and it takes NE (number of elements) steps to generate a mesh with NE elements. The new element sizes, δ_{new} at the current mesh are determined based on the error estimate on the FE solution. The adaptivity criterion is checked after specified number of iteration. The h-adaptive re-meshing is designed to keep the overall percentage velocity gradient norm error within prescribed tolerance. When the discretized error exceeds the tolerance, a new mesh is generated.

CHAPTER 6: RESULTS

6.1 Overview

The cross section of the Great Belt East Bridge (GBEB) suspension span was modeled using the adaptive finite element program. The GBEB cross section is illustrated in chapter 4, figure 4.1. As stated in previous chapters, the finite element program computes flow parameters: velocity, pressure and vorticity at each node in the computational domain. Then the program uses the computed pressure to compute forces acting on the bridge in the x direction and y direction (Fx and Fy). The computed forces are used to compute the coefficient of drag C_d, and coefficient of lift C_l according to equation 6.1 and 6.2.

$$C_d = \frac{F_x}{0.5\rho V^2 B} \tag{6.1}$$

$$C_l = \frac{F_y}{0.5\rho V^2 B} \tag{6.2}$$

B is the width of the bridge section, Fx and Fy are the drag and lift forces, V is the reference velocity and ρ is the density (Selvam, Bosch and Govindaswamy, (2003)). From chapter five, the width of the bridge is 31000mm. However, for ease of calculation, all dimensions are non dimensionlized with respect to the width of the bridge. Therefore B in this problem is taken as one.

The results of the fluid equations are written onto four output files: The first output file contains values of velocity, pressure and vorticity for each node at a particular time step when the grid is refined. The second output file contains values of velocity, pressure and vorticity for each node at the end of the computer run. The third output file

contains C_d and C_l at each time step. The fourth output file presents the x and y coordinates for each node and element connectivity information.

6.2 Fixed Grid

For this work, the results of five computer runs are reported. The input file used to generate the grid for each run was prepared following the instructions of the user manual presented in Appendix A. Input for the fixed grid program is comprised of the maximum overall velocity error for the region, total time of flow, viscosity, time step, minimum and maximum spacing of elements close to the bridge deck, number of time steps at which the adaptive is calling, x and y coordinates of boundary nodes, number of nodes and elements , boundary conditions for elements along the boundary and background element connectivity. A sample input file used to generate grid one of the five grids can be seen in Appendix B. For all runs, the flow is run for 60 sec and Reynolds number is 10^5. The time step is kept as 0.001, which means 1000 iterations are performed for a single unit of time. For each run, there were 60,000 iterations performed. This explains the intensive computational effort involved in the calculations.

The maximum grid spacing around the deck remains constant. Initial grid spacing at each boundary node can be seen in Appendix B.

From the five computer runs we were able to generate five grids. These five grids were generated using an automatic unstructured mesh generation algorithm with adaptive mesh refinement. The five grids are defined as Grid A-1, Grid A-2, Grid A-3, Grid B and Grid C.

For Grid A-1, Grid A-2 and Grid A-3, the unstructured triangular grids are generated by assigning a grid size of 0.1B away from the bridge section and a minimum

grid size of 0.001B near the bridge section. The grid sizes are non-dimensionalized with respect to the width (B=1) of the cross-section. The overall velocity gradient error over the region is specified in each grid.

For Grid B, the unstructured triangular grids are generated by assigning a grid size of 0.1B away from the bridge and a minimum grid size of 0.002B near the bridge section. Grid C is generated by assigning 0.1B away from the bridge and a minimum grid size of 0.003 B near the bridge section. In grids B and C, the overall velocity gradient error prescribed over the region is kept constant. Table 6.1 presents a summary of the grids generated in this research.

Table 6.1: Summary of Grids with spacing around the bridge deck.

Grid	Minimum Spacing around the GBEB Section (Hmin)	Maximum Spacing around the GBEB Section (Hmax)
A-1	0.001B	0.1B
A-2	0.001B	0.1B
A-3	0.001B	0.1B
B	0.002B	0.1B
C	0.003B	0.1B

All computations were performed using a personal computer and a Sun Microsystems Enterprise 4500 computer, with 8-400MHz/4Mb external cache CPU modules and 4 GB memory. The Sun Microsystems Enterprise computer was used for longer computer runs. The graphic visualizations of the grids and bridge program's data results are prepared by using the program Tecplot 8.0.

The main objective of this research is to validate the capacities and limitation of this improved finite element program. This is achieved by varying the overall velocity gradient error for a fixed grid configuration (Grid A-1, A-2, A-3) and by increasing the

minimum grid size near the bridge section while keeping the overall velocity gradient error constant (Grids B and C). The computed coefficient of drag (C_d), coefficient of Lift (C_l) and Strouhal number (S_t) are compared with wind tunnel experiments and other computational methods. In addition the pressure and vorticity contour plots are generated using Tecplot software.

6.3 Results

The velocity gradient error prescribed over each computational domain for grids A-1, A-2, A-3, B and C is illustrated in Table 6.2. Figure 6.1, 6.2 and 6.3 illustrates the grid generated for Grid A-1, Grid A-2, Grid A-3, respectively.

Table 6.2: Summary of grids with corresponding velocity gradient errors

Grid	Velocity Gradient Error (%)
A-1	25
A-2	30
A-3	35
B	27
C	27

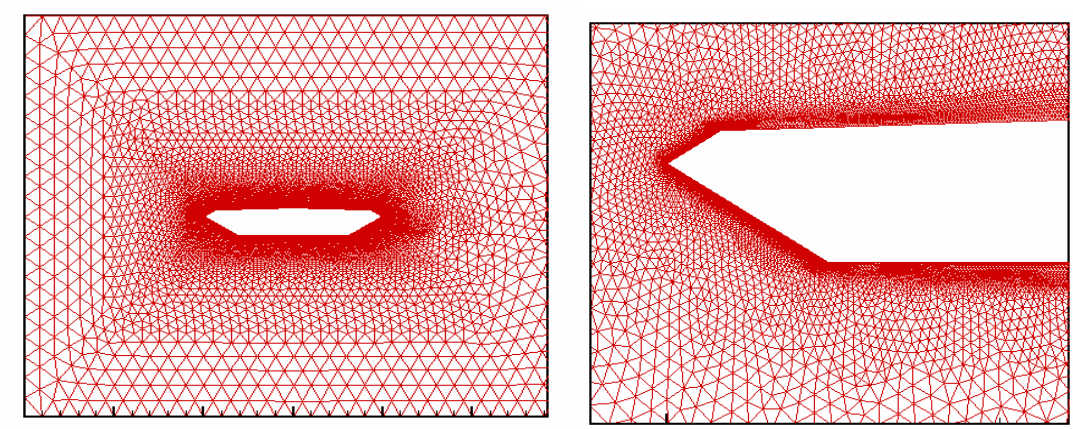

(a) Grid A-1 (b) Close up view of Grid A-1

Figure 6.1: GBEB suspension span for Grid A-1

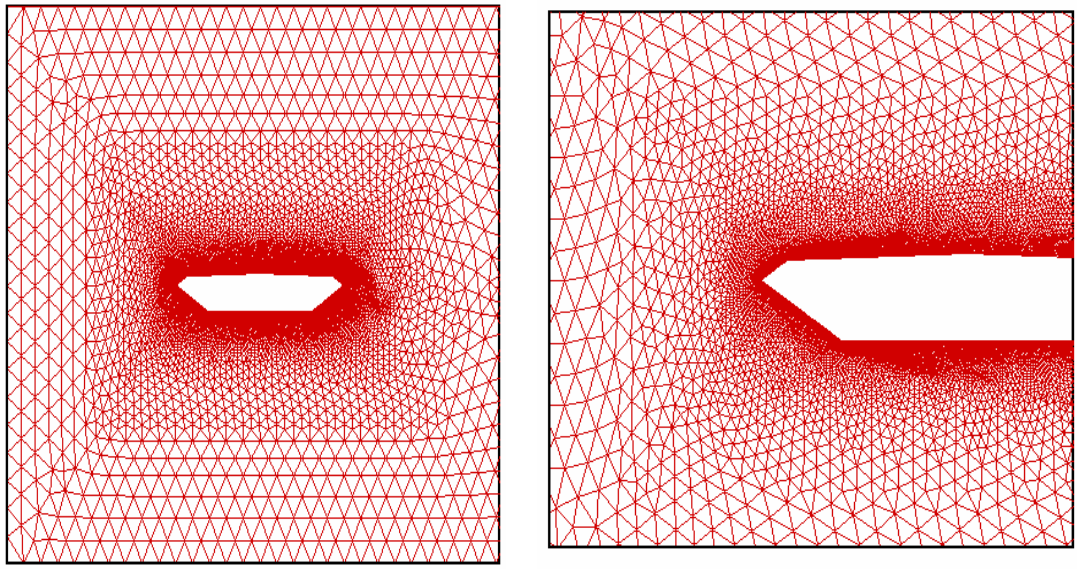

(a) Grid A-2 (b) Close up view of Grid A-2

Figure 6.2: GBEB suspension span for Grid A-2

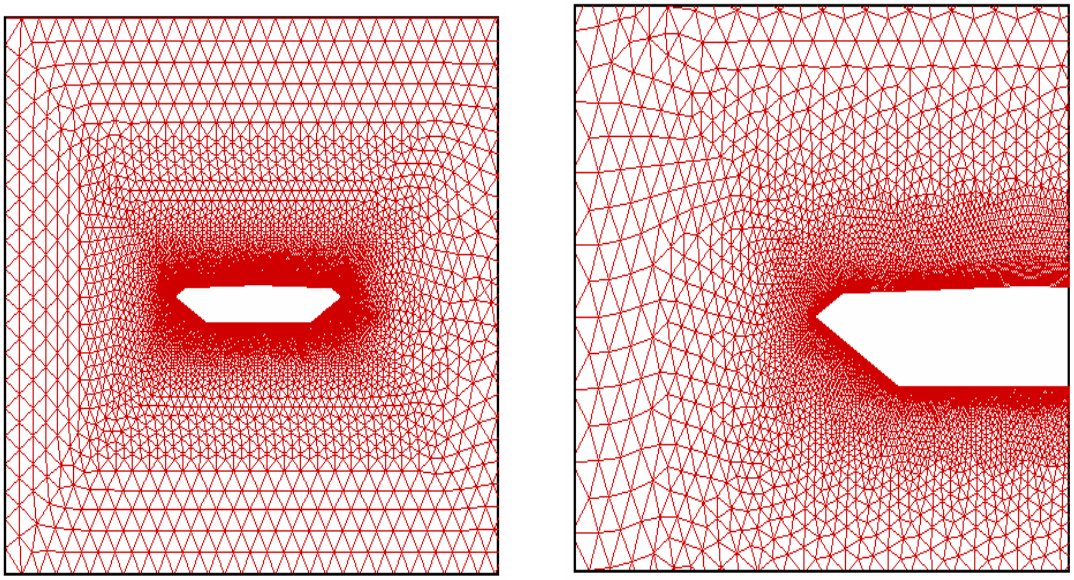

(a) Grid A-3 (b) Close up view of Grid A-3

Figure 6.3: GBEB suspension span for Grid A-3

As stated in section in 6.1, the computed forces in the x and y directions are used in equation 6.1 and 6.2 to compute the drag coefficient C_d and lift coefficient C_l. For each time step, the output is written onto a data file with the values for the coefficient of drag (C_d) and lift (C_l). The Strouhal number is computed for each run. The Strouhal number is computed according to equation 6.3.

$$S_t = \frac{H}{TV} \tag{6.3}$$

Where S_t = Strouhal number

H = Height of the bridge (non dimensionalized)

V = reference velocity (non dimensionalized)

T = period of oscillation of the lift forces

For our work, the non dimesionalized height of the bridge is 0.14 and the reference velocity is 1. To determine the period of the oscillation of the lift force, the frequency of oscillations of the lift force is plotted. Frequency (f) in this case equals 1/T. The peak value (frequency) from this plot is used in equation 3 to determine the Strouhal number (S_t). From the output file, the averaged C_d value is determined. The average C_d value and Strouhal number for each run is reported in the tables shown below.

Tables 6.3 and 6.4 shown below give the summary of the runs completed in this research.

Table 6.3: Summary of runs using a grid spacing of 0.001

Grid	Velocity Gradient Error (%)	Number of Refinement	C_d	S_t	Nodes	Elements
A-1	25	3	0.065	.123-.203	24089	46185
A-2	30	2	0.064	.171-.189	18260	34962
A-3	35	1	0.063	.189	13864	26229

Table 6.4: Summary of runs in relation to various grid configurations

Grid	Velocity Gradient Error (%)	Number of Refinements	Cd	St	Number of Nodes	Number of elements
B	27	6	0.061	0.231	18062	34985
C	27	4	0.055	0.244-.279	13160	25466

In Tables 6.3 and 6.4, the error in each grid is checked after the first 3100 iteration and then after every 15000 iteration thereafter. These two numbers are specified so that the adaptive process would be checked at intervals of approximately 5 seconds (non-dimensionalized time). The program refines the areas that have the most errors. In

our work, this would be the area near the bridge deck. Depending on the error prescribed in the input file, the program can run from a day to a few days.

From this research, we have found that the program only worked for errors prescribed at 25% or greater for grid sizes of 0.001 near the bridge deck. Several runs were made for grids with error less than 25%. These runs were not successful and are not reported in our results. However in Grids B and C, the lowest prescribed error that can be used in this model is 27% for grid sizes 0.002 and 0.003. Grid containing velocity error prescribed less than 27% for a 0.002 or 0.003 grid spacing near the bridge deck would not work in this model. From Table 6.4, it can be shown that a grid size of 0.002B around the bridge deck produced a higher coefficient of drag (C_d) and lower Strouhal number (S_t) than a grid size of .003B. However, running the program using a minimum grid size 0.002 took three times more computer time compared to running the program using minimum grid size of 0.003. Also Grid B refined 1.5 times more than grid C, hence producing a more accurate coefficient of drag (C_d) value

It is also found that a prescribed velocity error of 25% using a minimum size grid of 0.001 would produce a higher coefficient of drag (C_d) value in comparison with higher prescribed errors for the same grid size. In table 6.3, it can be shown that grid A-1 with 25% error refined more times compared to Grid A-2 and Grid A-3. However it takes more time to run Grid A-1 in comparison with other runs (A-2, A-3) with higher prescribed errors using the same minimum grid spacing around the bridge. In addition, Grid C refined twice as much Grid A-1 but produced a lower coefficient of drag (C_d) value because the velocity gradient error prescribed is 2% more than Grid A-1. Table 6.5

compares the C_d values of each run with wind tunnel values. From this table, grid A-1 has the least error in comparison with wind tunnel results.

Table 6.4: Comparison of computed Cd values with Wind tunnel

Grid	Cd	Wind tunnel Cd	Error(%)
A-1	0.065	0.077	16
A-2	0.064	0.077	17
A-3	0.063	0.077	18
B	0.061	0.077	21
C	0.055	0.077	29

As mentioned the first output file is written onto a file in which values of velocity, pressure and vorticity for each node is presented. After each run the pressure contours, vorticity contours for each grid were generated using Tecplot software.

6.4 Vorticity Contour Plots

The nose of the bridge deck section causes the incoming flow to separate. The separation of flow generates vortices (spiral motions of wind) that are carried along the deck surfaces by a mean flow's velocity. In the previous works, Selvam et al (2001) using the quadrilateral elements could not develop the vortices on the top deck due to limitation of grid resolution. This can be shown in figure 6.4. In this work, we are able to develop and visualize the built of vortices above and below the bridge deck in Figs. 6.5 - 6.7. The recirculation effect of the vorticity is more visible in figure 6.5 for Grid A-1 compared to Grid A-2 or A-3. Grid A-1 being the more refined grid was able to capture better recirculation features of vorticity on the top of the bridge deck.

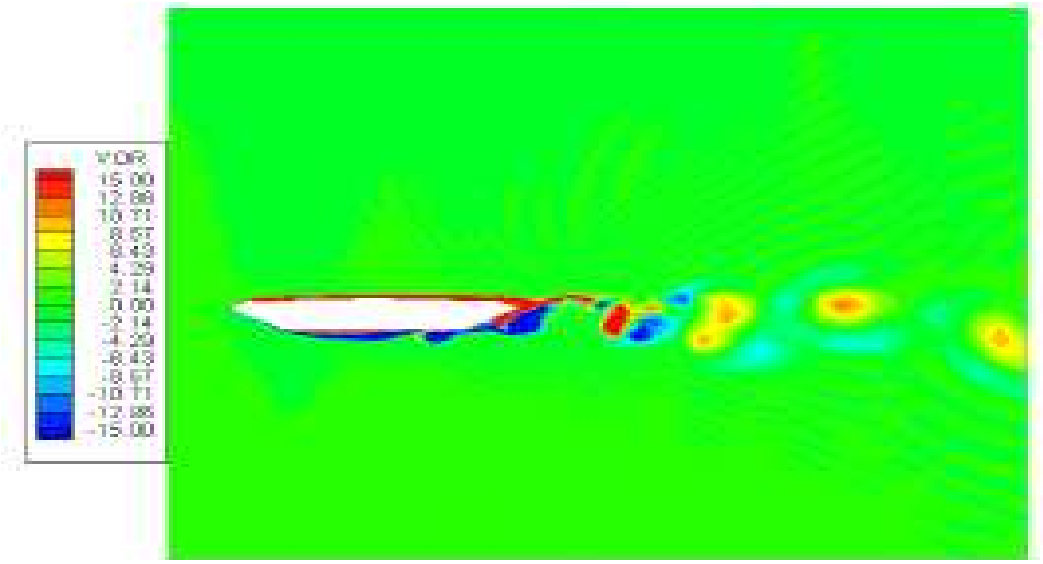

Figure 6.4: Vorticity Contour Plot for grid spacing 0.001 (Selvam and Govindaswamy, 2001)

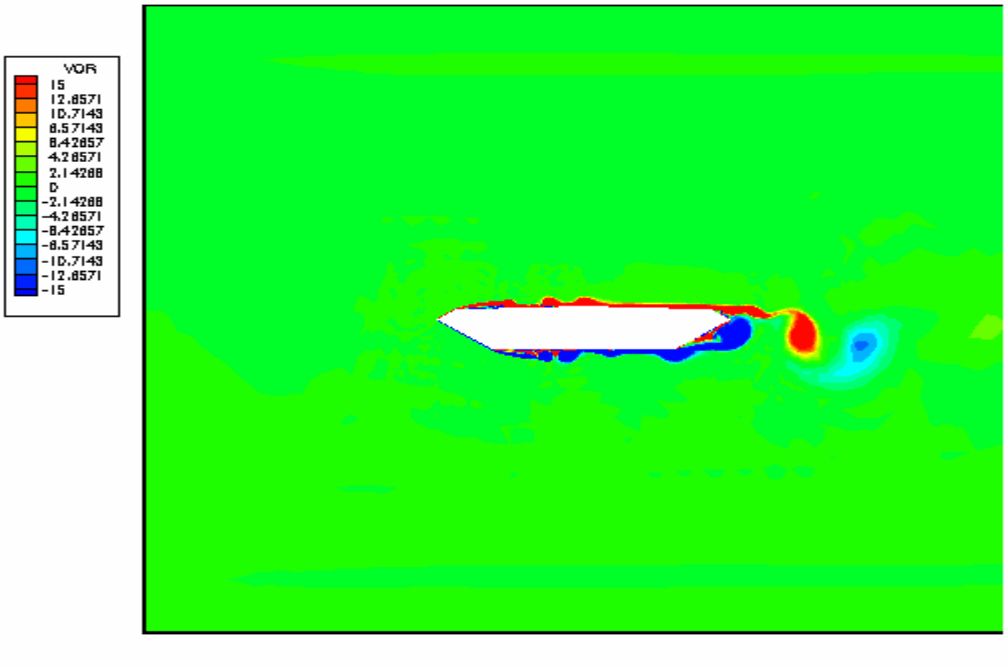

Figure 6.5 Vorticity Contour for Grid A-1

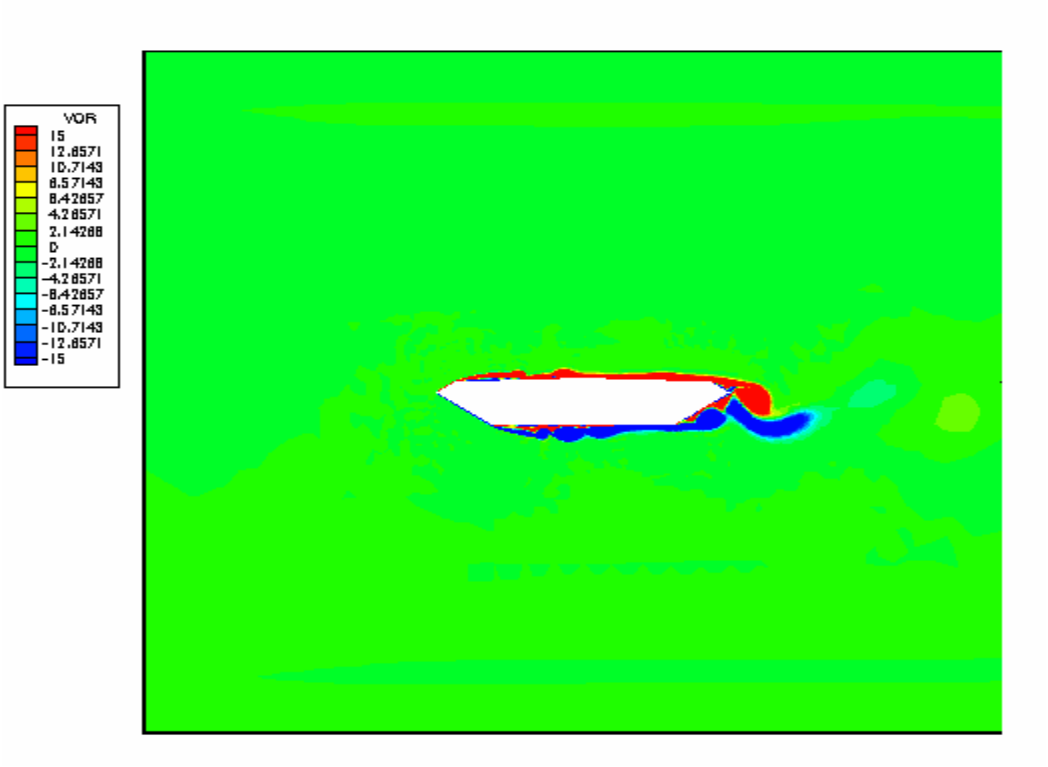

Figure 6.6 Vorticity Contour for Grid A-2

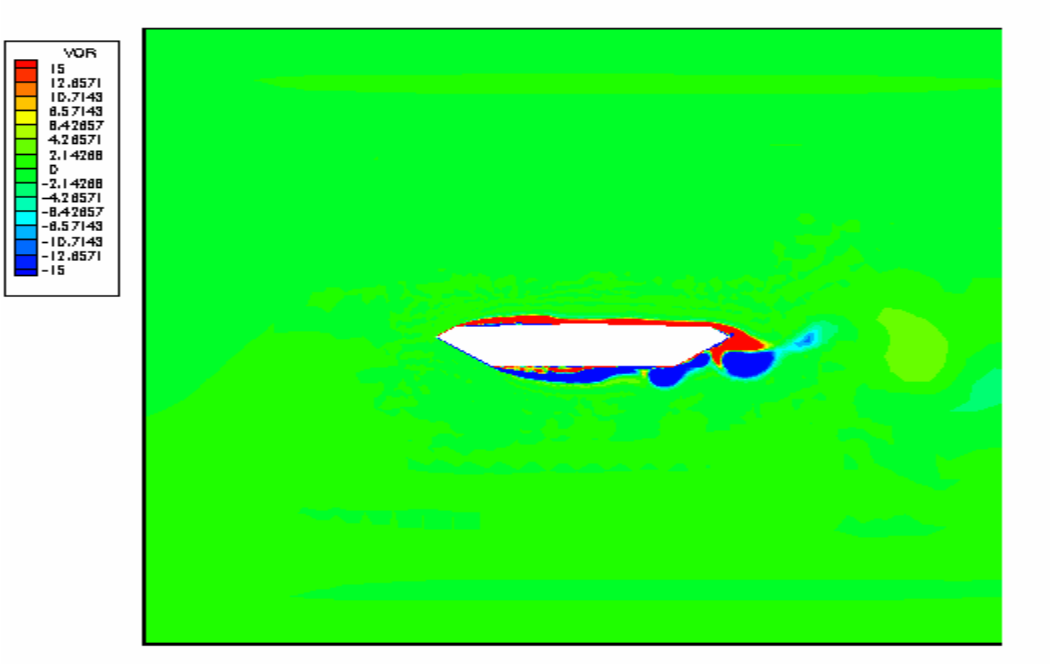

Figure 6.7 Vorticity Contour for Grid A-3

6.5 Pressure Contour Plots

Previously, Selvam et al. (2001) using quadrilateral elements found that for a grid size of 0.001B around the bridge deck, the pressure distribution at the top of the deck was not easily visible. Figure 6.8 illustrates the pressure contour plot for a grid size of 0.001B generated by Selvam and Govindaswamy (2001). With the h-adaptive program, the grid resolution around the bridge deck was improved. Therefore we are able to visualize more variation of pressure (positive and negative pressures) on the top deck of the bridge section in Figure 6.9 (grid with adaptive) compared to Figure 6.8 (grid without adaptive). The distribution of pressure shown in Figures 6.8 and 6.9 is between .50 and -1.50. Figures 6.10 - 6.12 illustrates the pressure distribution around the bridge deck for Grids A-1, A-2 and A-3. The range of pressures shown in Figures 6.10 - 6.12 is between .25 and -1.4. The pressure contours vary according to the change in the density of the grid and the prescribed velocity error **.**The positive pressure (orange regions) and suction forces (green regions) around the bridge deck are shown as a result of the formation of vortices on the top the bridge deck. In figure 6.10, the grid is more refined and has the least velocity gradient error therefore there is better variation of pressure around the bridge deck in Figure 6.10 than in Figure 6.11 and Figure 6.12.

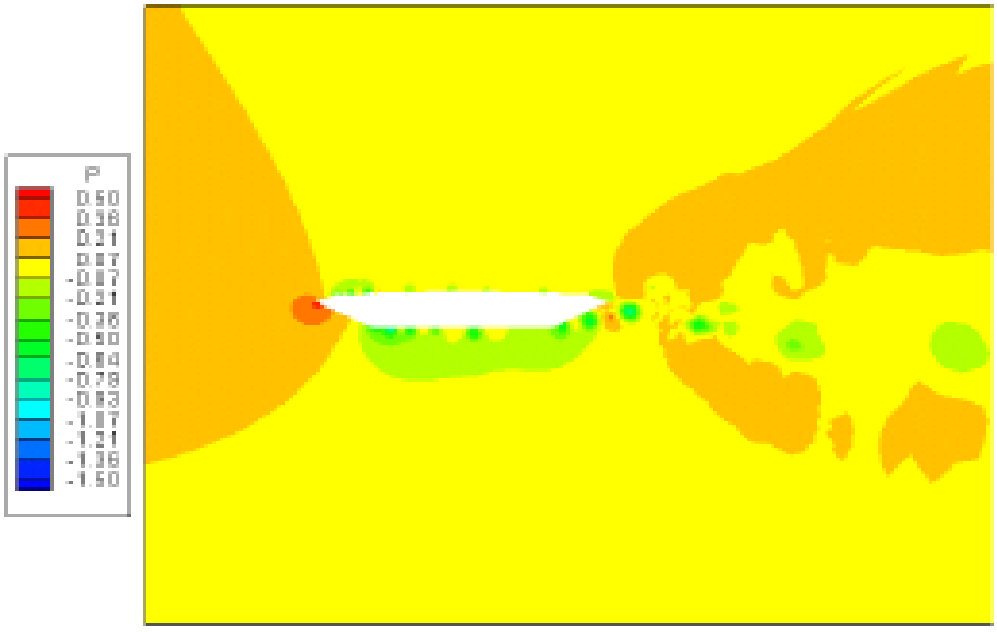

Figure 6.8: Pressure Contour for grid size 0.001(Selvam, 2001)

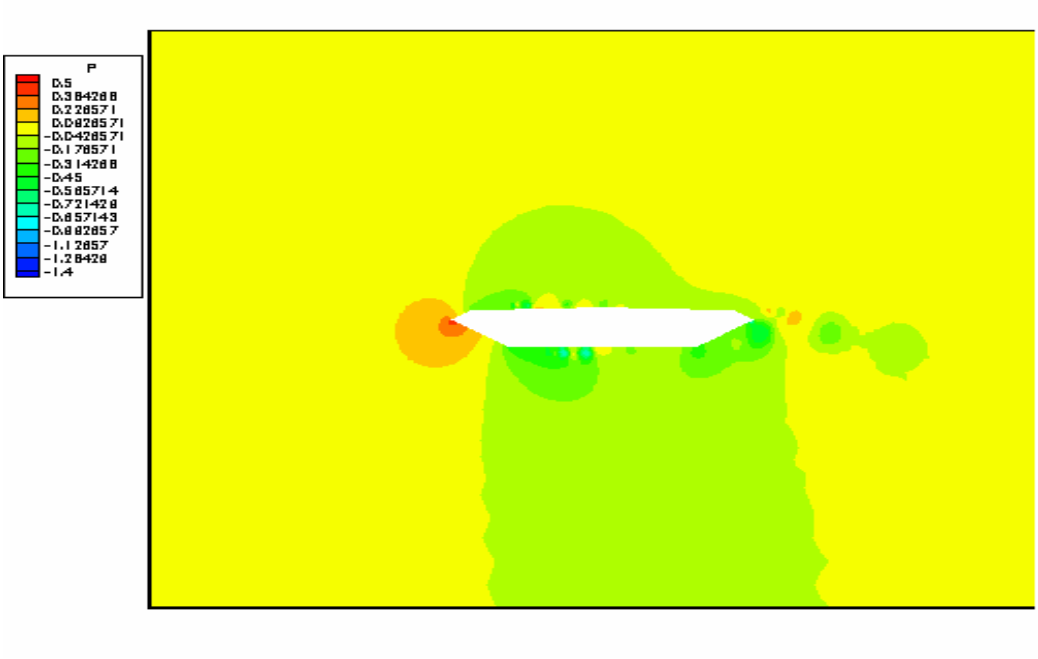

Figure 6.9: Pressure Contour for Grid A-1

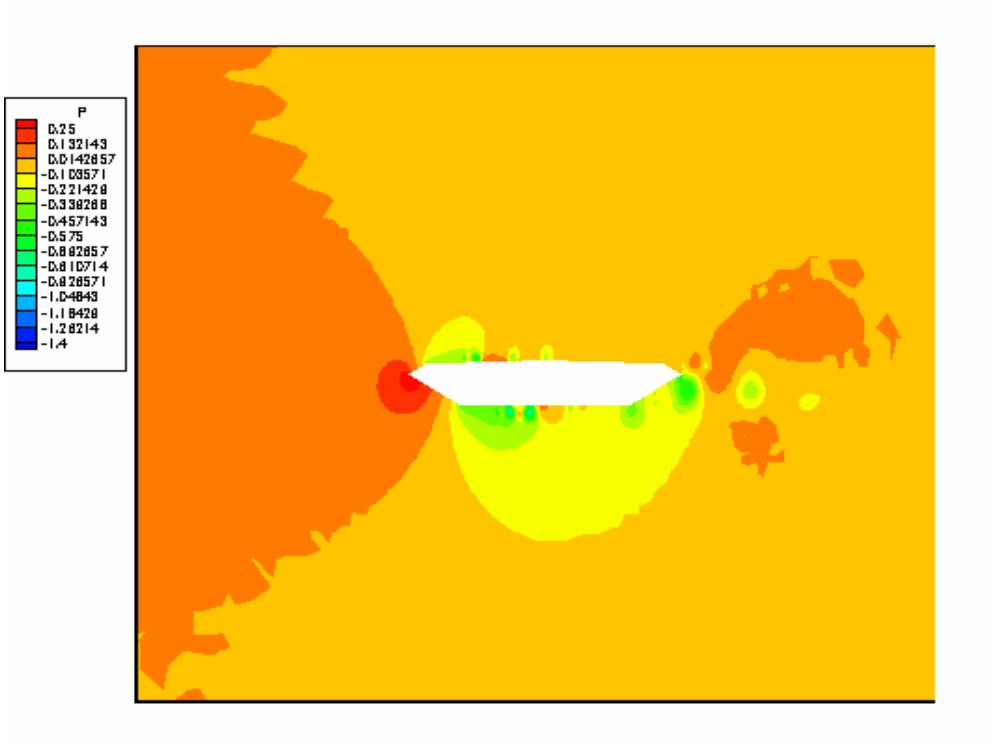

Figure 6.10: Pressure Contour for Grid A-1

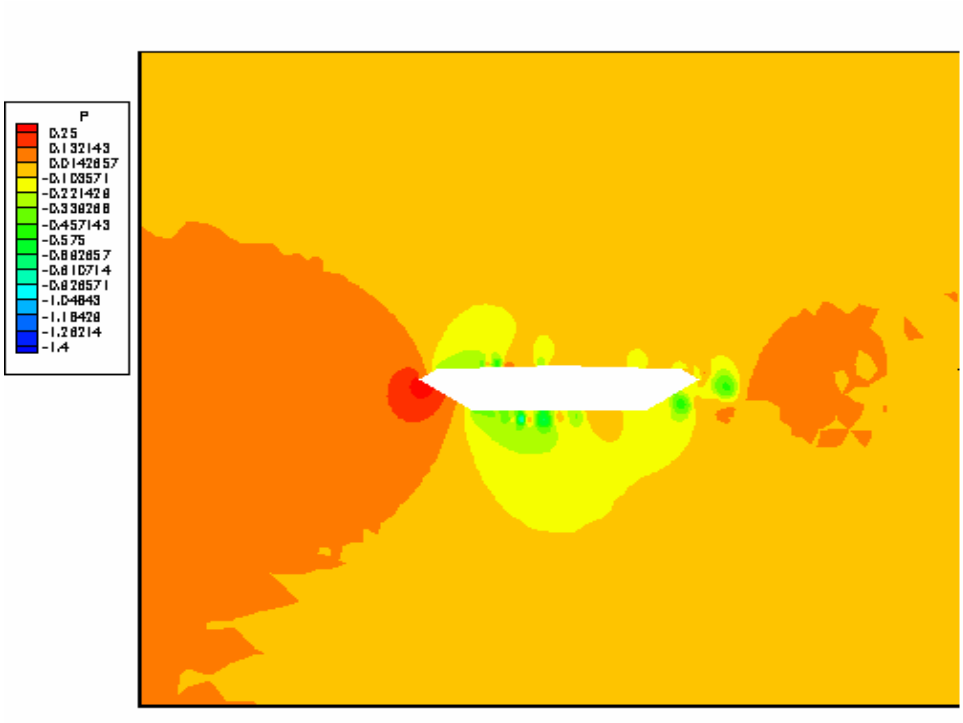

Figure 6.11: Pressure Contour for Grid A-2

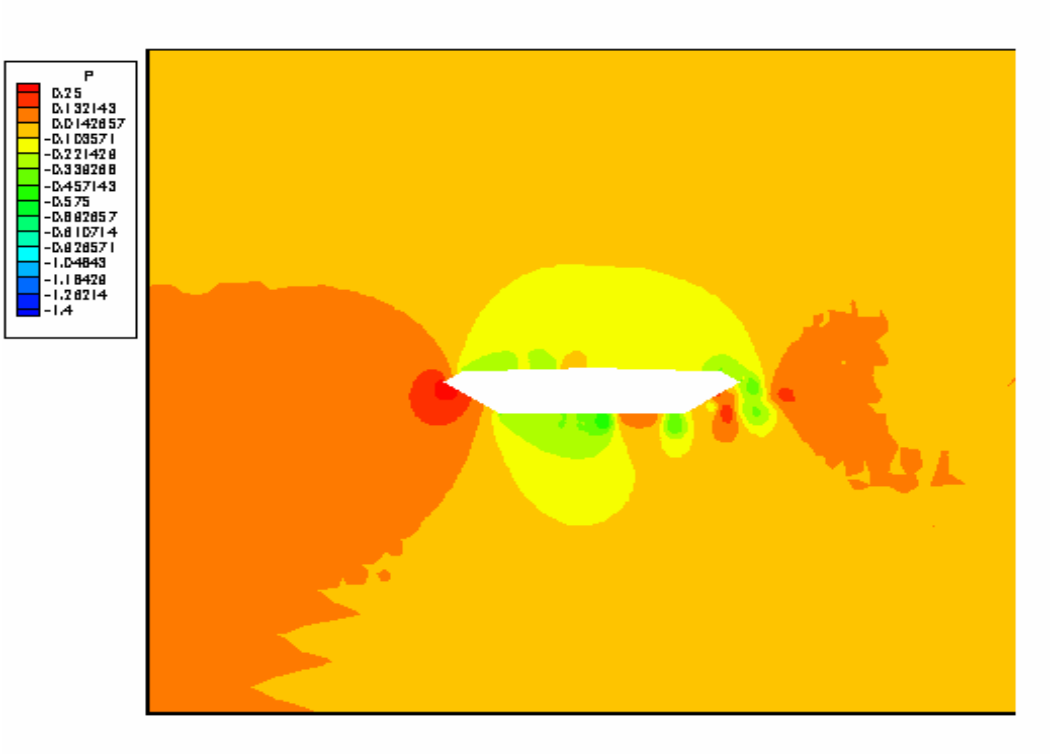

Figure 6.12: Pressure Contour for GridA-3

6.6 Drag and lift Charts

The variation of drag coefficient (C_d) and lift coefficient (C_l) as a function of time is plotted using the Tecplot software. The results for Grid A-1, A-2 and A-3 are shown in Figures 6.13-6.15. It is observed that there is better variation (positive and negative) of drag and lift coefficients in Figure 6.13 compared to the variation of drag coefficients in Figure 6.14 and Figure 6.15. As flow past a bridge section, it experiences a variation of positive and negative pressures on the surface of the bridge deck. In Figure 6.15, the drag coefficient is mostly negative which does not reflect he true variation of drag over the bride section.

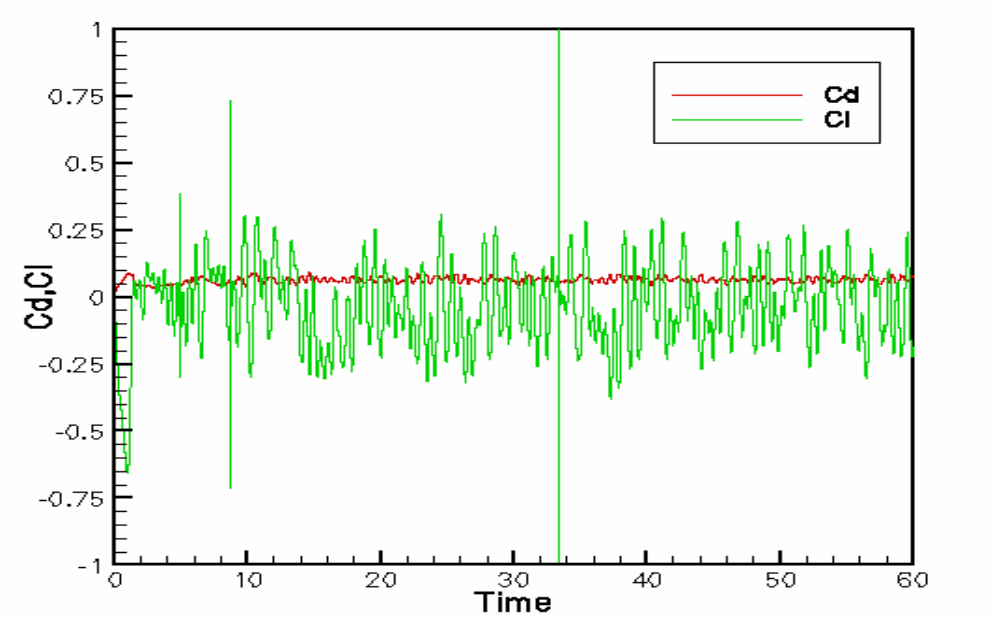

Figure 6.13: Drag and Lift coefficients Vs Time for Grid A-1

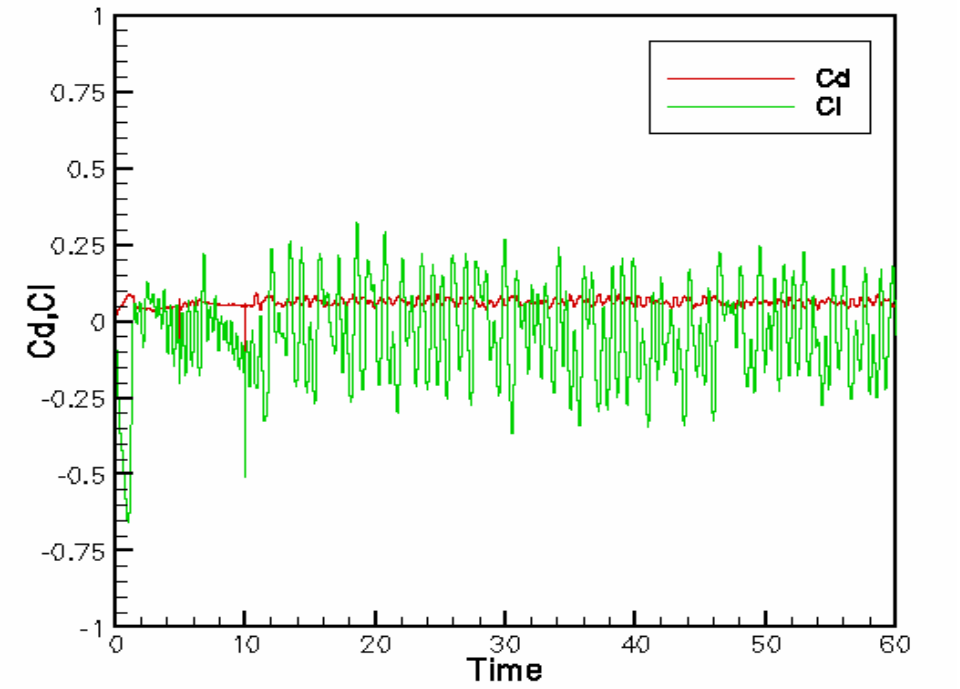

Figure 6.14: Drag and Lift coefficients Vs Time for Grid A-2

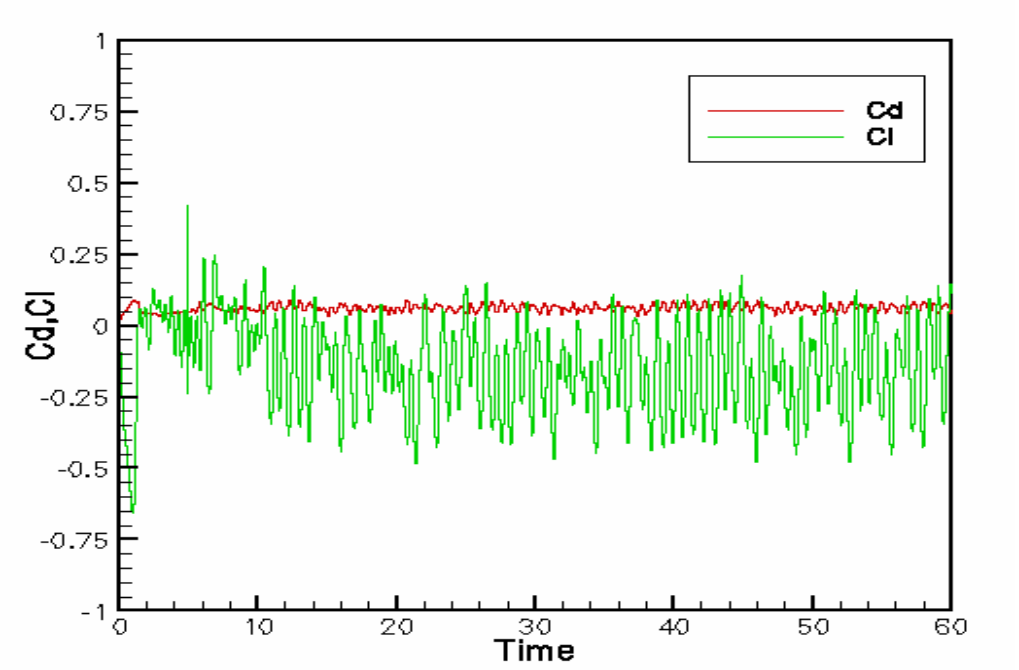

Figure 6.15: Drag and Lift coefficients Vs Time for Grid A-3

6.7 Comparison of Flow Parameters

The results of the work done by other researchers for the same GBEB suspension span are presented below. The coefficient of drag and the Strouhal number are comparable with wind tunnel results. Time averaged C_d and S_t values are compared to wind tunnel results of Larsen (1997) and Taylor (1999) and computational results of Selvam and Govindaswamy (2001 and 2002).

Table 6.5: Comparison of the drag coefficient and Strouhal number obtained from numerical simulations and wind tunnel tests (Fixed case).

Model by	**Cd**	**St**
This work (25%)	0.065	0.123-.203
Selvam Govindaswamy(2003)	0.062	0.140
Larsen et al (1997)	0.061	0.100-0.168
Taylor et al (1999)	0.050	0.16-0.18
Wind Tunnel Experiments	0.077	0.109-0.158

From the table 6.5, the C_d value computed by Selvam and Govindaswamy (2001) was 0.061, 20% lower than wind tunnel result. In this work, using the h–adaptive technique, the C_d value was improved to 0.065. This is 16% lower than the wind tunnel results. In addition the Strouhal number computed in previous works is 0.14 and in this work (0.123-.203). The Strouhal number was improved slightly.

CHAPTER 7: CONCLUSION

7.1 Summary

Selvam and Govindaswamy (2001) created two finite element models. These computer models were used to compute flow parameters using quadrilateral finite elements (structured meshes). The main problem with this existing model was creating a proper grid around the bridge section and controlling the error within the solution.

To address this problem, automatic generated triangular grids (unstructured grids) are used in the current model. Adaptive Finite Element techniques are used in the model to refine the grid and control the error in the solution. Error estimation algorithms determine the error in the FEM mesh and adaptive techniques remesh the grid around the bridge section when the calculated error exceeds a specified limit.

In the updated model, adaptive h- refinement procedures are used to refine the grid based on a adaptivity criterion. The adaptivity criterion is based on an estimate of error in the velocity gradients. This adaptive re-meshing technique allows the overall percentage velocity gradient norm error to fall within a prescribed tolerance.

The objective of this research was to evaluate the influence of velocity gradient errors on accuracy of results. First, three grids were generated with specified velocity errors 25%, 30% and 35% respectively. The computed Strouhal number and drag coefficient for these grids were studied and compared to wind tunnel and other relevant computational simulation experiments. In addition two other grids were generated varying the grid spacing around the bridge deck and keeping the prescribed velocity gradient constant. The computed Strouhal number (S_t) and drag coefficient (C_d) for these

two grids were studied and compared to wind tunnel and other relevant computational simulation experiments.

From this research, we have found that for the program only works for velocity gradient errors prescribed 25% or greater using a grid sizes 0.001 or less. It is also found that a prescribed velocity error of 25% using a minimum size grid of 0.001 would produce a more accurate C_d value in comparison with higher prescribed errors for the same grid size. For grid sizes (0.002 - 0.003) around the bridge, the lowest prescribed error that can be used in this model is 27%. Smaller grid spacing produced more accurate results and took more time to run.

The C_d value computed by Selvam and Govindaswamy (2001) was 0.061, 20% lower than wind tunnel result (0.077). In this work, using the h-adaptive FEM program, the C_d value was improved to 0.065. This is 16% lower than the wind tunnel results. In addition the Strouhal number computed in previous works is 0.14 and in this work (0.123-.203).

7.2 Advantages and Disadvantages

The advantage of using adaptive finite element is that it reduces the operating time needed to create an efficient grid. In addition it was shown to produce more accurate results than non adaptive finite element models. By using adaptive techniques, aerodynamic analyses can be performed in about two weeks using a personal computer (costs less than $1000)

One limitation of using adaptive finite element is that i for grid spacing higher than 0.001 a prescribed error of 25% does not work. From the previous chapters, it is found that very finer discretization is required around the bridge to capture the flow

features. The present unstructured grid necessitates very large number of nodes and elements to capture the boundary layer. This results in the use of more computer memory.

7.3 Recommendations for Future Work

- Future work should be done using the adaptive program with different bridge cross- sections.
- A combination of adaptive techniques such as h-p refinement can be used to refine the FEM grid to produce more accurate results.

REFERENCES:

Anderson, J. D. Jr, "**Fundamentals of Aerodynamics**" third edition , publisher : Mc Graw Hill Companies 2001

Babuska I., T.Strouboulis, C.S.Upadhyay, S.K.Gangaraj, and K.Copps, "Validation of a posteriori error estimators by numerical approach", **International Journal for Numerical Methods in Engineering,** 37(1994), 1073-1123

Brooks**,** A.N., T.J.R.Hughes, "Streamline unwind/Petrov-Galerkin formulations for convection dominated flows with particular emphasis on the incompressible Navier-Stokes equations", Computer Methods in Applied Mechanics and Engineering, 32(1982), 199-259

Bowers, N.A., **"Tacoma Narrows bridge wrecked by wind**", Engineering News Record (1940,)**,** Vol.125, pp.647

Cengel, Y. A. "**Fluid Mechanics: fundamentals and applications /Yunus A. Cengel"**, John M. Cimbala. – 1st edition McGraw –Hill

Choi, C.K. and W.J.Yu, "Adaptive refinement/recovery for analysis of wind around structure", **Journal of Aerospace Engineering**, 12(1999), 168-175.

Enevoldsen, I., Hansen, S.O., Kvamsdal, T., Pedersen, C., Thorbek, L.t., 1999, "Computational wind simulations for cable-supported bridges", in Larsen, A., Larose, G.L. and Livesey, F.M. (eds), **Wind Engineering into the 21st Century**, A.A. Balkema, Rotterdam, Vol. 2, 1265-1270.

Farren, Henry J. **" Wind and Earthquake Response in Very Long Span Cable-Stayed and Suspension Bridges"**, Fall 1999, page 55-60

Frandsen, J.B. and McRobie, F.A., 1999, "Computational aeroelastic modeling to guidelong-span bridge cross-section design", in Larsen, A., Larose, G.L. and Livesey, F.M. (eds), **Wind Engineering into the 21st Century,** A.A. Balkema, Rotterdam, Vol. 2, 1277-1284.

Gazel A.,W., 2004 **"Validation of aeroelastic finite element program for two dimensional flow past suspended bridges using moving grids",** MS Thesis, Department of Civil Engineering, 4190 Bell Engineering Center, University Of Arkansas, Fayetteville, AR 72701, May 2004

Gamble, S. "Wind Tunnel Testing – A Breeze through" **Structures magazine**, November 2003, pages 24 -27

George, P.L., "Automatic mesh generation: Application to finite element methods", John Wiley & sons (1992)

Huston, D.R. and Bosch, H.R., 1996, "Aerodynamic Design of Highway Structures" **Public roads On – line**, "http;//www.tfhrc.gov/pubrds/winter96/p96w46.htm

Larsen, A. and Walter, J.H., 1996. "A New computational method for assessment of the aeroelastic stability of long span bridges", **IABSE**, Copenhagon

Lo, S. H. (1985). "A new mesh generation scheme for arbitrary planar domains." ***International Journal for Numerical Methods in Engineering,* 21**, 1403-1426.

Morgenthal, G. "Numerical Analysis of Bridge Aerodynamics" March 2006, **fib Journal Structural Concrete** pages 35-41

Peraire, J., Vahdati, M., Morgan, K., and Zienkiewicz, O. C. (1987). "Adaptive remeshing for compressible flow computations." **Journal of Computational Physics**, **72**, 449-446.

Peraire, J., Morgan, K., and Peiro, J., **"Unstructured Mesh Methods in CFD, I.C. report 90**-04 , June 1990, dept of Aeronautics, Material College of Science and Technology and Medicine, London.

Selvam R.P, "Computation of flow over circular cylinder using p-adaptive FEM, International Symposium on Wind and Structures for the 21st Century", Chejudo, Korea, January 26-28, (2000)

Selvam, R.P., Govindaswamy, S. and Bosch, H., Aeroelastic analysis of bridge girder section using computer modeling, Final report: MBTC FR-1095, **Mack-Blackwell National Rural Transportation study center**, University of Arkansas, 2001

Selvam, R.P., Govindaswamy, S. and Bosch, H. (2002), Aeroelastic analysis of bridges using FEM and moving grids, *Wind & Structures*, **5**, 257-266

Selvam, R.P. and Qu, Z.Q., Adaptive p-finite element method for wind engineering, **Wind & Structures**, Vol. 5, pp. 301-316, 2002

Selvam, R. P., Qu, Z. Q. (2003). "Aeroelastic analysis of bridge deck sections by FEM using LES (Part 4) – Software for generation of unstructured grids." **Final Report, Lendis Corporation.**

Selvam R.P. and Patro S.K, Aeroelastic analysis of bridge deck sections by FEM using LES Software for FEA using unstructured grids, Yearly Progress Report: **LENDIS Corporation**, University of Arkansas, 2006

Selvam R.P. and Patro S.K, Aeroelastic analysis of bridge deck sections by FEM using LES Software for FEA using unstructured grids, Yearly Progress Report: **Final LENDIS Corporation**, University of Arkansas, 2007

Selvam R.P., S. Govindaswamy and Harold Bosch " Computation of flutter Velocities for Bridges Using FEM, CFD and Moving grids" in **ASCE Sructures** 2001

Zienkiewicz, O.C. and Zhu, J. Z. (1987). "A simple error estimator and adaptive procedure for practical engineering analysis." **International Journal for Numerical Methods in Engineering**, **24**, 337-357.

Zienkiewicz, O. C. (2006). "The background of error estimation and adaptivity in finite element computations." **Computational Methods in Applied Mechanics and Engineering**, **195**, 207-213.

APPENDIX A:

USER MANUAL FOR H-ADAPTIVE FINITE ELEMENT PROGRAM

USER MANUAL FOR H-ADAPTIVE GRID GENERATION PROGRAM - af2d-2.f

This user manual describes details for preparation of input data for the h adaptive bridge calculations.

1. Read Control Data 1

READ (2,*) ETA1, ETA2, TIME1, VISC, DTIME, HMIN, HMAX

ETA1 : Overall percentage error

ETA2 : Percentage error in the non-singularity area

TIME1 : Total Time

VISC : Viscosity = 1/Reynolds's number

DTIME : Time step

HMIN : Specified Minimum size of element

HMAX : Specified Maximum size of element

2. Read Control Data 2

READ (2,*) INODE, NISEG, NBACK, NPOIN, NOUT, NOUT2

INODE : Number of Input Nodes

NISEG : Total Number of input line segments to define the boundary

NBACK : Number of triangles in the background grid

NPOIN : Number of point in the background grid

NOUT : Number of time steps at which adaptive is calling

NOUT2 : Second number of time steps at which adaptive is calling

3. Read x & y coordinates of the domain

READ (2,*) ((COORD (I, J), I =1, 2), J=1, INODE)

Each row give x and y of the specified computational geometry from 1- INODE

4. Give the node numbers for the boundary segments

READ (2,*) ((MISEG (I, J), J=1, 3), I=1, NISEG)

Here each row gives first node, second node and boundary information for NISEG lines. Here numbers 1 to 5 can be used for boundary information to identify different boundary segments. Using these numbers one can implement the boundary conditions in the finite element program.

The segment numbers should be numbered in such a way that the discretized region should be always on the left of the traversed direction.

5. Background grid information

READ (2,*) ((CBACK (I, J), J=1, 3), I=1, NPOIN)

Each row specifies that the x and y coordinates of the background grid and the size of the grid around the node expected. This information of x, y and grid size should to be continued for NPOIN rows.

6. Connectivity of the background grid

READ (2,*) ((MBACK (I, J), J = 1, 3) I=1, NBACK)

Each row indicates the three nodes that make the background triangle. Node numbers should be counter clockwise direction in each row. Number of rows should continue for NBACK (Number of Background triangles)

This program produces the following output files. The details of the output files are as follows.

A2dp- A.plt This contains x, y, vx, vy, p, and vor at a certain time (i.e. time at which adaptive is necessary)

A2dp.plt	This contains x, y, vx, vy, p, and vor at the end of total time
A2dg.plt	This contains time, cd, and cl at each time level
Grid-o.plt	This contains “x” and “y” coordinates for each node and connectivity of each element. This also gives the number of nodes and elements within the grid.

Where

x, y	x and y coordinates of node
vx, vy	x and y components of velocity
p	pressure
vor	vorticity

Note: Adaptive is necessary when error is not within specified permissible limit.

APPENDIX B:

SAMPLE INPUT FILE

```
0.25 60.0 1.0e-05 0.001 0.001 .1
13   13   16   16          3000 15000
-1   1
-1  -1
 7  -1
 7   1
0.71774   0.037702
0.93548   0.032258
1         0
0.80645   -0.096774
0.19355   -0.096774
0         0
0.06452   0.032258
0.28226   0.037702
0.5       0.043145
1  2  3
2  3  4
3  4  5
4  1  2
5  6  1
6  7  1
7  8  1
8  9  1
9  10 1
10 11 1
11 12 1
12 13 1
13 5  1
-1    1    0.1
-1   -1    0.1
 7   -1    0.1
 7    1    0.1
 2    1    0.1
 2   -1    0.1
0.71774   0.037702   0.005
0.93548   0.032258   0.005
1         0          0.005
0.80645   -0.096774  0.005
0.5       -0.096774  0.005
0.19355   -0.096774  0.005
0         0          0.005
0.06452   0.032258   0.005
0.28226   0.037702   0.005
0.5       0.043145   0.005
 1    2   13
13    2   12
```

12 2 11
11 2 6
11 6 10
10 6 9
9 6 5
9 5 8
8 5 7
7 5 16
16 5 1
16 1 15
15 1 14
14 1 13
4 5 6